60-GHz Transmission Link Using Uni-Traveling Carrier Photodiodes at the Transmitter and the Receiver

Ahmad Wasfi Mohammad , Haymen Shams , *Member, IEEE*, Chin-Pang Liu , *Member, IEEE*, Chris Graham , Michele Natrella, Alwyn J. Seeds , *Fellow, IEEE*, and Cyril C. Renaud , *Senior Member, IEEE*

Abstract—We present the first demonstration of a wireless transmission link based on uni-traveling carrier photodiodes (UTC-PDs) as transmitter and receiver. In this demonstration, a UTC-PD was used at the transmitter to generate a 1-Gbps ON–OFF keying data signal at a carrier frequency of 61.3 GHz by heterodyning two modulated optical tones originating from an optical frequency comb system. The generated electrical heterodyne signal was transmitted, using a 25-dBi gain parabolic antenna. An identical antenna was used to detect the signal at the receiver, followed by an optically pumped UTC-PD mixer to down-convert the received RF signal to an intermediate frequency of 6.3 GHz, which was subsequently amplified and acquired by a real-time oscilloscope for offline processing. The recovered data showed an open eye diagram, and a bit error rate of the order of 10^{-5} was measured. The receiver UTC-PD was characterized in terms of its conversion loss and noise figure (NF), and the overall NF of the receiver was measured at 21.5 dB.

Index Terms—5G mobile communication, millimetre wave technology, photodiodes.

I. INTRODUCTION

THE Global mobile data traffic is expected to reach 49 Exabyte per month by 2021, which is a 7-fold increase compared to 2016 [1]. Such a dramatic increase in data traffic will be impossible to cope with using the current 4G technologies, especially with the rapid rise of new applications that require very low end-to-end latency in Machine to Machine (M2M) communications and the Internet of Things (IoT) [2], which will account for about 29% of connected devices in 2021 [1]. Consequently, the International Telecommunication Union (ITU) has defined a set of requirements for the next generation of mobile communication systems (5G) in terms of data rate, capacity, latency, quality of service (QoS), and energy efficiency [3].

The 5G network is expected to deliver speeds of the order of Gbps. Hence, it cannot rely on the current low frequency bands (<3 GHz) as they do not offer wide enough bandwidth to support such high data rates, and are almost fully occupied by other communication systems, such as mobile, broadcast and satellite services [4]. As a result, researchers have been exploring millimetre waves (MMWs) because of the abundance of spectrum in the MMW range (30 GHz–300 GHz) which will allow for high speed communications even at low spectral efficiency. Another advantage of moving to the MMW range is that at such high frequencies the antenna size becomes smaller, and it becomes practical to develop integrated antenna arrays [5] and enjoy the benefits of the massive multiple input multiple output (MIMO) [6]. Moreover, the high propagation losses in the MMW range limit the effective communication distance to about 200 m [7], making it more secure and allowing for more frequency reuse.

MMW generation is a research area that involves two competing technologies: electronics and photonics. With the electronic techniques, MMWs can be generated directly from high frequency diode- or transistor- based sources or indirectly from a low frequency source followed by frequency multiplication stages [8]. The issue with the latter approach is that it can be costly and complex to implement [9]. On the other hand, photonic techniques can generate high data rate, low phase noise, and spurious free signals [10] with ultra-wide tunability, and can be easily integrated with the existing fiber networks where transmission loss is low [11].

Several photonic techniques for MMW generation have been demonstrated, including [12], [13]: photomixing (optical heterodyning) with two laser diodes, optical frequency combs (OFC), direct intensity modulation, optical external modulation, mode locked laser diodes (MLLD), nonlinear effects in waveguides and fibers, and Brillouin fiber lasers. These methods use a photodiode for the optical to electrical conversion, by which it generates an electrical signal at a frequency that is defined by the spacing between the optical tones, as mathematically explained in [9]. In this context, the uni-traveling carrier photodiode (UTC-PD) is commonly used at frequencies above 100 GHz because of its superior performance as a MMW emitter in terms of high emitted power and the high bandwidth (−3 dB bandwidths of

A. W. Mohammad, H. Shams, C.-P. Liu, C. Graham, A. J. Seeds, and C. C. Renaud are with the Ultrafast Photonics Group, Department of Electronic and Electrical Engineering, University College London, London WC1E 7JE, U.K. (e-mail: ahmad.mohammad@ucl.ac.uk; h.shams@ucl.ac.uk; chin.liu@ucl.ac.uk; c.graham@ucl.ac.uk; a.seeds@ucl.ac.uk; c.renaud@ucl.ac.uk).

M. Natrella is with the Leonardo MW Ltd, Airborne & Space Systems Division, Luton LU1 3PG, U.K. (e-mail: m.natrella@alumni.ucl.ac.uk).

up to 310 GHz have been demonstrated using this type of photodiode) [14].

MMW receivers typically comprise an antenna to detect the radiation, a low noise preamplifier to boost the signal power and increase the receiver sensitivity, and, finally, an MMW detector, which can be a direct or a heterodyne detector [15]. While direct detection is based on diode rectification (envelope detection), heterodyne detection is based on mixing the received signal with a local oscillator (LO) to down-convert it to a low intermediate frequency (IF) [16]. Superconductor–insulator–superconductors (SIS), hot electron bolometers (HEB) and Schottky diode mixers are common detectors [8]. Recently, the UTC-PD has been demonstrated as an optically pumped mixer at frequencies up to 600 GHz [17]. However, this demonstration used an unmodulated signal with only 100 Hz of IF detection bandwidth which is not enough for communications purposes.

An UTC-PD mixer offers important advantages compared with currently available mixers. For example, unlike SIS and HEB mixers that typically require cooling to low temperatures, a UTC-PD mixer works at room temperature. Also, it offers very wide frequency tuning up to sub-terahertz frequencies without requiring an electronic LO, which is a limitation in Schottky mixers. Finally, the UTC-PD can be monolithically integrated with lasers and modulators on InP substrates [18] and easily integrated with fiber networks as it is optimized to work in the optical communications window at 1550 nm.

The 60 GHz band is particularly interesting for 5 G because it contains at least 7 GHz of unlicensed spectrum in many countries [19] which allows for multi-Gbps communications. However, the presence of oxygen absorption peak at 60 GHz, attenuates the signal power significantly (15 dB/km) in this frequency band [5]. Also, heavy rain results in additional attenuation due to scattering, since raindrops are of a similar size to the wavelength of the MMW signal [5]. Furthermore, 60 GHz signals cannot penetrate concrete walls [20]. Consequently, the 60 GHz band is more suitable for short distance indoor communications. Potential applications in this frequency band include: HD video streaming, file transfer, and wireless Gigabit Ethernet [19].

In a previous work [21], we demonstrated a UTC-PD-based wireless receiver at 33.5 GHz. In this work, we present the first demonstration of MMW transmission link based on UTC-PDs in the transmitter and the receiver. We realized a 61.3 GHz wireless transmission link implementing a UTC-PD at the transmitter for MMW signal generation, by heterodyning two modulated optical tones originating from an OFC system. Optical signal modulation was realized using a Mach-Zehnder modulator (MZM) driven by a 1 Gbps on-off keying (OOK) signal. The 61.3 GHz signal was transmitted wirelessly using a 25 dBi gain parabolic antenna before being detected by an identical receiver antenna. At the receiver, a UTC-PD was pumped by optical tones from two free running lasers spaced by 55 GHz to down convert the received signal to an IF of 6.3 GHz, where it was captured for offline processing.

The recovered data showed an open eye diagram, and a bit error rate (BER) of the order of 10^{-5} was measured. The conversion loss and noise figure (NF) performance of the receiver UTC-PD mixer are also presented.
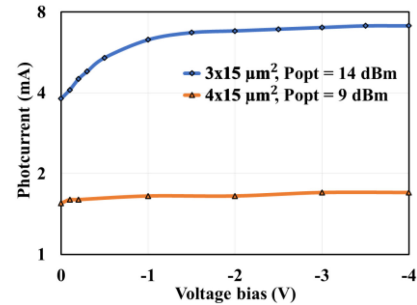

Fig. 1. The photocurrent versus bias voltage characteristics for the UTC-PDs at the transmitter ($3 \times 15\ \mu m^2$) and the receiver ($4 \times 15\ \mu m^2$).

This experiment demonstrates the capabilities of the UTC-PD as an emitter and a detector of MMWs, which is an important step towards realizing photonic integrated transmitters and receivers. In fact, the UTC-PD has already been integrated with lasers, electro-optical modulators, and semiconductor optical amplifiers (SOAs) on a single photonic integrated circuit (PIC), and has been successfully demonstrated as a photonic integrated MMW transmitter in a 100 Mbps wireless link at 90 GHz [22]. The findings of our experiment show that the same PIC could be used as a MMW detector, and this would establish that a photonic integrated transceiver is feasible, which will offer a low-cost, high data rate and energy efficient solution for 5G.

The rest of the paper is organized as follows. Section II shows UTC-PDs characterization results in terms of photocurrent responsivity and frequency response. Also described are the opto-electronic mixing procedure in the receiver UCT-PD, its conversion loss optimization, and its NF measurement. In Section III, we describe the experimental system for the transmitter and the receiver in detail, and present the experimental results as well as the NF measurements of the entire receiver. Finally, we conclude this work in Section IV.

II. UTC-PD CHARACTERIZATION

The UTC-PD based transmission link presented in this work uses two UTC-PDs: The first UTC-PD, which has dimensions of $3 \times 15\ \mu m^2$, uses optical heterodyning to generate the MMW at the transmitter, while the second UTC-PD, which has dimensions of $4 \times 15\ \mu m^2$, is used as an opto-electronic mixer at the receiver. The epitaxial structure of the devices is detailed in [23].

First, both UTC-PDs were characterized in terms of their photocurrent for different values of voltage bias, while the optical power injected into the UTC-PDs was fixed at 14 dBm and 9 dBm for the transmitter UTC-PD and the receiver UTC-PD, respectively. The photocurrent versus voltage bias is plotted in Fig. 1. It gives responsivities of 0.28 A/W and 0.2 A/W at −4 V for the transmitter and receiver UTC-PDs, respectively.

Then, the frequency response of the devices was measured using the heterodyne system shown in Fig. 2, where optical signals from two free running lasers were coupled and injected into the UTC-PDs. The spacing between the two optical signals was swept from zero to 67 GHz, while the generated electrical
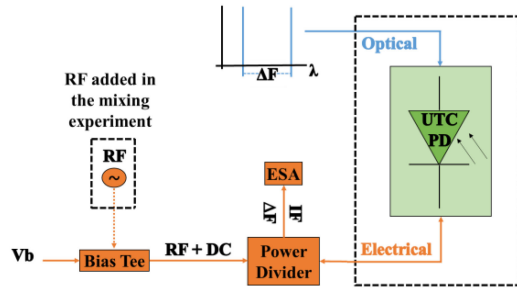
Fig. 2. System for optical heterodyning (without RF) and optoelectronic mixing (with RF) in UTC-PD.
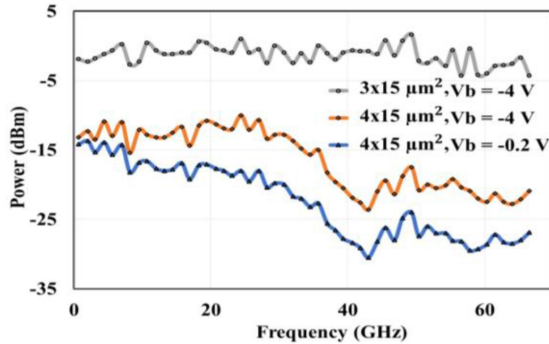

Fig. 3. Frequency response of the transmitter and receiver UTC-PDs.

Fig. 4. Dependence of IF power on frequency for the receiver UTC-PD.

Fig. 5. Finding the optimum bias point for the UTC-PD mixer at 6.3 GHz IF.

heterodyne signals were extracted by a coplanar waveguide probe and measured using an electrical spectrum analyzer (ESA). The frequency responses of the devices are plotted in Fig. 3 at a voltage bias of −4 V (the figure also shows the frequency response of the receiver UTC-PD at a voltage bias of −0.2 V, which gives the optimum conversion loss as will be shown next).

The frequency response curves give 3 dB-bandwidths of more than 60 GHz and 35 GHz for the transmitter and receiver UTC-PDs, respectively. This difference in bandwidth is attributed to the difference in the devices dimensions.

Next, the optoelectronic mixing characteristics of the receiver UTC-PD were studied using the system shown in Fig. 2, by applying a 61.3 GHz signal - from a signal generator - with a power of −11 dBm as measured at the input of the UTC-PD probe. Optical tones from two free running lasers were injected into the UTC-PD, and their spacing was swept between 50.3 GHz and 61.3 GHz, and the power of the generated IF was measured (Fig. 4), which is a down-converted version of the RF signal at a frequency equal to the difference between the RF and generated electrical heterodyne. Fig. 4 shows that mixing efficiency depends on IF, and that relatively high mixing efficiency occurs at 6.3 GHz.

The difference between the power of the incoming RF signal at the input of the UTC-PD and the power of the generated IF define the conversion loss of the UTC-PD mixer. As shown in [24], the conversion loss is a function of the bias voltage and the power of the optical LO. To find the optimum conversion loss for this mixer, the voltage bias was swept from zero to −4 V while the optical LO power was fixed at 9.8 dBm, and the power of the 61.3 GHz RF was set to −11 dBm as measured at the
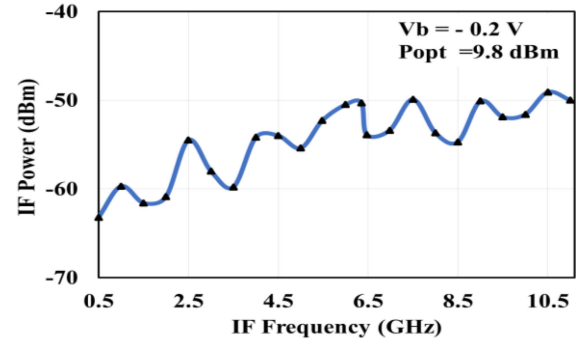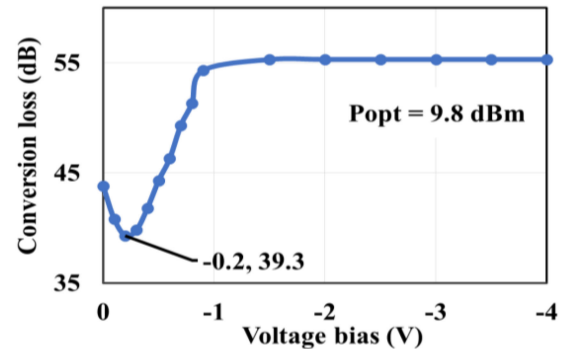
input of the UTC-PD probe. Results are plotted in Fig. 5, which shows that minimum conversion loss (39.3 dB) is obtained at −0.2 V, which is the point of maximum nonlinearity in the I-V curve in Fig. 1. This is in agreement with the findings of [24] that best mixing occurs at maximum differential conductance. However, Fig. 5 exhibits a different behavior at higher bias voltage compared to that in [24] due to the different epitaxial structure of the UTC-PD used in this work.

Finally, the UTC-PD opto-electronic mixer was characterized in terms of its NF using the NF equation [25]:

$$NF = N_o - G(-174) \qquad (1)$$

where N_o refers to the noise power density generated by the UTC-PD measured in dBm/Hz, G refers to the gain of the UTC-PD mixer (negative conversion loss) in dB, and finally the −174 dBm/Hz term is the thermal noise power spectral density at 290 K. The "Noise Meas" function in ESA was used to measure N_o at 6.3 GHz both when the optical LO was OFF and ON. An LNA (gain = 32.8 dB) was added after the UTC-PD to amplify the UTC-PD generated noise to increase the measurement accuracy. The optical LO was turned off at first, and N_o was measured for the ESA noise floor and the LNA combined (N_o_OFF = −140.7 dBm/Hz). Then, the optical LO was switched on, and the new N_o was measured (N_o_ON = −137.4 dBm/Hz). Then, N_o for the UTC-PD alone was calculated by subtracting N_o_OFF and the LNA gain from N_o_ON in linear units. At the optimum bias point (−0.2 V), a NF of 40.36 dB was measured at an IF of 6.3 GHz.
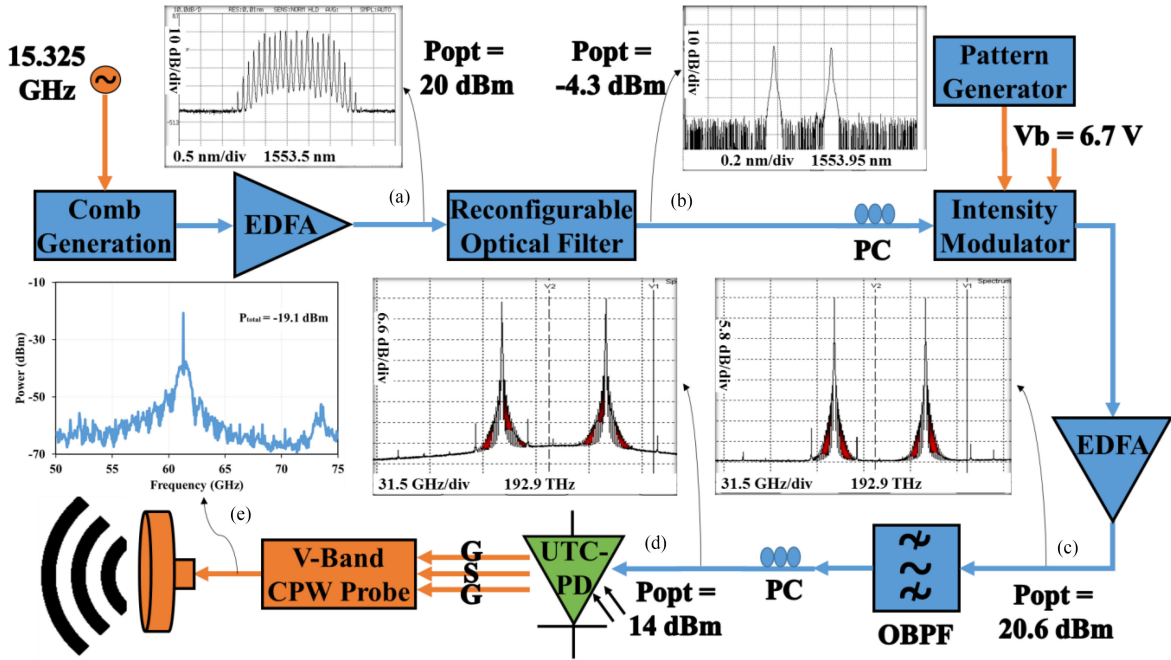
Fig. 6. Block diagram of the transmitter showing: (a) the optical spectrum of the OFC (RBW = 0.01 nm), (b) two selected comb lines with 61.3 GHz spacing (RBW = 0.01 nm), (c) the two comb lines after modulation and amplification (RBW = 140 MHz), (d) the optical spectrum at the input of the lensed fiber (RBW = 140 MHz), and (e) the electrical spectrum of the generated MMW signal at the input of the transmitter antenna (RBW = 300 kHz).

III. A 60 GHz UTC-PD Based Transmission Link

A. Transmitter Setup

The block diagram of the transmitter is shown in Fig. 6, where a non-return-to-zero (NRZ) 1 Gbps OOK pseudo random bit sequence (PRBS) data signal with a length of $2^{11} - 1$ was emitted at 61.3 GHz by the $3 \times 15 \, \mu \, \text{m}^2$ UTC-PD by heterodyning two modulated optical tones originating from an OFC system.

The OFC system generated a comb of lines centered at 1553.5 nm and spaced by 15.325 GHz, as shown in Fig. 6(a). The comb was amplified by an erbium doped fiber amplifier (EDFA) with a constant output power of 20 dBm followed by a reconfigurable optical filter (Waveshaper) to select two optical lines spaced by 61.3 GHz (4×15.325 GHz) while suppressing all the other lines (suppression ratio > 37 dB), as shown in Fig. 6(b). The total power of the two-tone optical signal at the output of the reconfigurable filter was measured at −4.3 dBm. An MZM, biased at $V_b = 6.7$ V, was used to modulate the two optical tones with a 1 Gbps OOK data signal generated by a pattern generator. After that, the optical signal was amplified by an EDFA (output = 21 dBm). The optical spectrum of the modulated optical tones after amplification is shown in Fig. 6(c), and the total power at the output of the EDFA was measured at 20.6 dBm. The EDFA was followed by a 1 nm-wide optical bandpass filter (OBPF) to reduce the amplified spontaneous emission (ASE) noise. Finally, the optical signal was coupled to a lensed fiber to illuminate the UTC-PD. The total power of the optical signal at the input of the lensed fiber was measured at 14 dBm, and the optical spectrum at this stage is shown in Fig. 6(d).

The UTC-PD generated electrical heterodyne signal at 61.3 GHz, which was extracted by a V-band (50 GHz–75 GHz) coplanar waveguide probe with an integrated bias Tee applying a voltage bias of −4 V. A 60 GHz V–cable was used to send the extracted 61.3 GHz signal to the transmitter antenna, which is of the parabolic type with a gain of 25 dBi at 61.3 GHz. The electrical spectrum of the transmitted signal is shown in Fig. 6(e), and the total power of the signal at this stage was −19.1 dBm. The signal was transmitted over 0.55 m of wireless distance (limited by the physical space available) before reaching the receiver antenna, which is identical to the transmitter antenna.

B. Receiver Setup

The block diagram of the receiver system is shown in Fig. 7. It implements a UTC-PD in an optically pumped mixer configuration to down-convert the incoming 61.3 GHz data signal to a lower 6.3 GHz IF.

The optical LO was generated from two free running external cavity lasers spaced by 55 GHz. As shown in Fig. 7, the two optical tones were coupled using an optical coupler, amplified by an EDFA (output = 17 dBm), filtered by an OBPF and injected into the UTC-PD using a lensed fiber. The total power of the optical signal at the input of the lensed fiber was measured at 9.8 dBm, and the optical spectrum at this stage is shown in Fig. 7(a).

The total power of 61.3 GHz data signal at the receiver antenna was −35.4 dBm (Fig. 7(b)). The received signal was amplified by a low noise amplifier (LNA) (gain = 35.9 dB, NF = 2.2 dB) followed by a bias Tee to provide the voltage bias (−0.2 V) to the UTC-PD. A DC to 65 GHz power divider was used to allow for the simultaneous supply of the RF signal to the UTC-PD and the extraction of the IF from the UTC-PD. The signal at the input of the receiver UTC-PD probe is shown in Fig. 7(c), and its total power was measured at −6.6 dBm.

The extracted IF signal from the power divider was then amplified (gain = 35.4 dB, NF = 1.9 dB) and, finally, captured
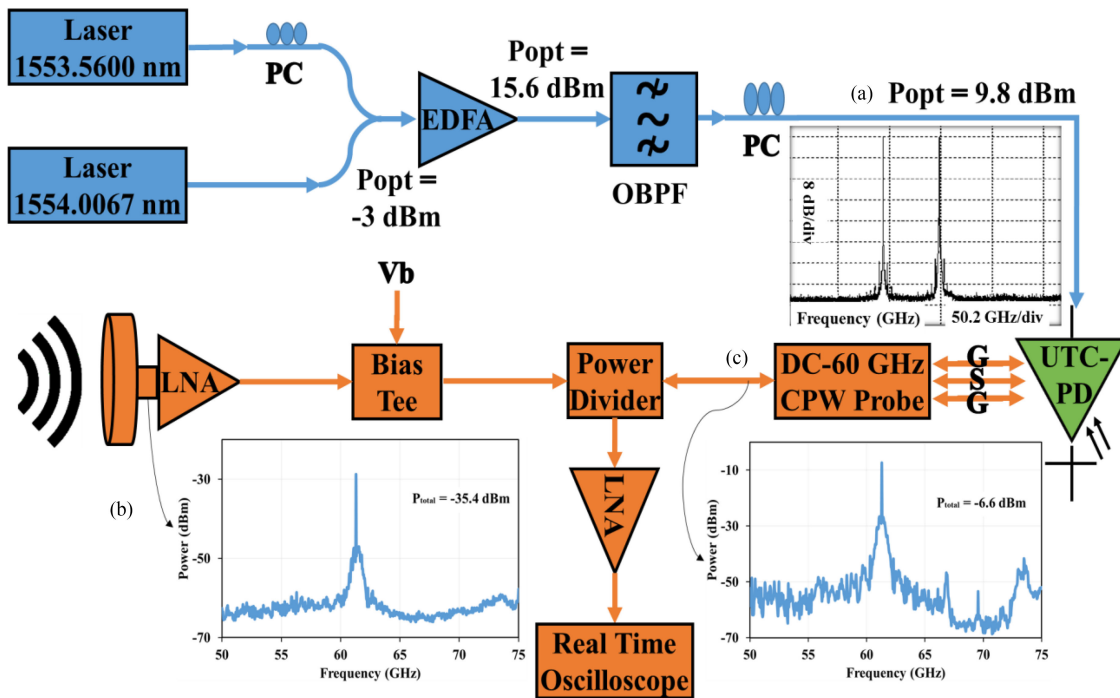
Fig. 7. Block diagram of the receiver showing: (a) the optical spectrum at the input of the lensed fiber (RBW = 140 MHz), (b) the electrical spectrum of the MMW signal at the output of the receiver antenna (RBW = 300 kHz), and (c) the electrical spectrum of the MMW signal at the input of the receiver UTC-PD probe (RBW = 300 kHz).
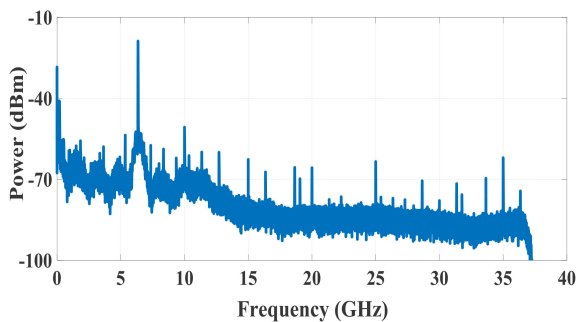

Fig. 8. The electrical spectrum of the amplified IF signal (RBW = 100 kHz).
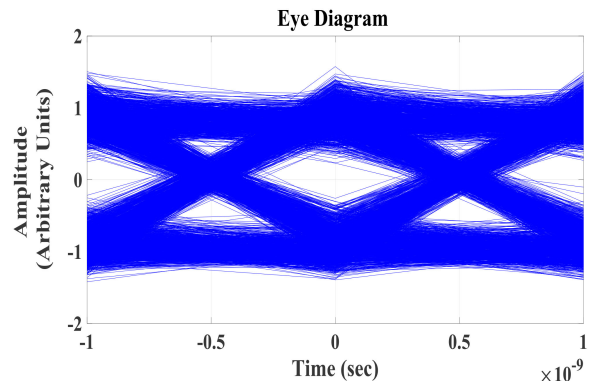

Fig. 9. An eye diagram representation of the recovered data after equalization.

by the real-time oscilloscope (RTO) for off-line processing. The RTO has a bandwidth of 36 GHz and a sampling rate of 80 Gsamples/second, and the length of the captured waveform is 10 μs, which is equivalent to 10,000 bits. The electrical spectrum of the acquired waveform is shown in Fig. 8.

The offline digital signal processing (DSP) includes the following steps: signal filtering, digital down-conversion to the baseband, channel equalization using constant modulus algorithm (CMA), and envelope detection [26].

The recovered data produced an open eye diagram, as shown in Fig. 9. The number of errors in the recovered data was counted and found to be zero in a 10,000-bit transmission. To obtain more precise results, transmission was repeated 35 times, which corresponds to 350,000 bits, and the total number of errors obtained was 3, corresponding to BER of the order of 10^{-5}, which will allow for error-free transmission when forward error correction (FEC) is employed.

In this experiment the transmission distance was limited to 0.55 m, partly due to the absence of a power amplifier at the transmitter. In order to achieve longer transmission distances a similar experiment was conducted using $4 \times 15\,\mu m^2$ and $3 \times 15\mu m^2$ UTC-PDs at the transmitter and the receiver, respectively, with a power amplifier installed at the transmitter (gain = 43 dB, NF = 0.9 dB). In the new setup the transmitter and the receiver antennas were intentionally misaligned to emulate a longer transmission distance. The distance between the antennas was 0.58 m, and extra attenuation introduced by antenna misalignment was measured at 38.7 dB which is equivalent to 86-fold increase in distance (d_{new} = 50 m). The recovered data showed zero errors in a 10,000-bit transmission. Transmission was repeated 11 times, which corresponds to 110,000 bits, and the number of errors was zero, which suggests a BER of less than 10^{-5}.

TABLE I
NF AND GAIN/LOSS MEASUREMENTS FOR THE COMPONENTS IN THE RECEIVER

Stage	Gain (dB)	NF (dB)
RF LNA	35.9	2.2
Passive elements in RF path (bias Tee, power divider, cable, connectors)	-16.5	0
UTC-PD mixer	-39.3	40.36
Passive elements in IF path (power divider, cable, connectors)	-12.7	0
IF LNA	35.4	1.9

Finally, all the components in the receiver were characterized in terms of their gain/loss and NF. A summary of these measurements is provided in Table I. Then, Friis formula [27] was used to calculate the receiver's overall NF:

$$F_{tot} = F_1 + (F_2 - 1)/G_1 + (F_3 - 1)/G_1 G_2 + \dots \quad (2)$$

where F_{tot} is the total NF of the receiver, F_n and G_n are the NF and the gain of the nth stage, respectively. Calculations give an overall NF of 21.5 dB for the receiver.

The data rates demonstrated in this paper were limited to 1 Gbps. This is partly due to the weak modulation depth of the MZM at the transmitter, which resulted in a low-power data signal (Fig. 6(e)), and this limited the SNR of the generated signal, and so, the data rate. Amplifying the data signal at input of the MZM could help increase the modulation depth and the data rates. Also, the current configuration of the receiver can be optimized to allow for longer transmission distances and higher data rates. For example, the receiver implements a DC-65 GHz power divider to allow for the simultaneous supply of RF and the extraction of IF signals. However, this introduces losses to both signals and deteriorates the SNR. Further, it limits the operating frequency to 65 GHz. These limitations can be overcome by redesigning the waveguides of the receiver UTC-PD to create separate paths for RF and IF signals. Another major limitation is the high conversion loss of the UTC-PD mixer (39.3 dB), which requires further studies on optimizing its epitaxial structure to enhance its mixing efficiency, which will increase the sensitivity of the receiver and allow for higher data rates.

As a final remark, although this setup is not optimized it demonstrates a proof of concept of mixing in UTC-PD and how it can be useful in wireless receivers. In that regards, it was verified that mixing took place in the UTC-PD, and not somewhere else, like an LNA, for instance. This is because the optoelectronic mixing experiment described in Fig. 2 does not implement an LNA. Also, the frequency of the down-converted signal in Fig. 8 was tunable by adjusting the spacing between the two optical tones driving the receiver UTC-PD, and the power of this signal was dependent on the voltage bias on the receiver UTC-PD following the behavior shown in Fig. 5.

IV. CONCLUSION

We successfully demonstrated a 1 Gbps OOK and a potentially 50 m long wireless link at 61.3 GHz implementing UTC-PDs at the transmitter and the receiver. While the transmitter UTC-PD was driven by coherent optical tones from a frequency comb system, the receiver UTC-PD was driven by two free running lasers, featuring a simple and widely tunable receiver.

The current configuration of the receiver is partly limited by the power divider which introduces losses in the RF and the IF paths, and limits the operating frequency of the receiver to 65 GHz. These limitations can be overcome by redesigning the waveguides of receiver UTC-PD such that RF supply and IF extraction are done using two different probes.

This proof of concept experiment was done using non-integrated components. As a future work, it is planned to integrate these components on a photonic chip, which could offer a low-cost, high data rate and energy efficient solution for 5G and future networks. Furthermore, this photonic based solution offers advantages compared to the existing electronic receivers, such as the low cost (as it does not require an electronic LO), the wide tunability, and the easy integrability with the existing fiber networks.

REFERENCES

[1] Cisco, Cisco Visual Networking Index: Global Mobile Data Traffic Forecast Update, 2016–2021 White Paper. [Online]. Available: http://www.cisco.com/c/en/us/solutions/collateral/service-provider/visual-networking-index-vni/mobile-white-paper-c11-520862.html. Accessed on: Mar. 29, 2017.

[2] P. Schulz et al., "Latency critical IoT applications in 5G: Perspective on the design of radio interface and network architecture," IEEE Commun. Mag., vol. 55, no. 2, pp. 70–78, Feb. 2017.

[3] ITU-R, Draft new Report ITU-R M. [IMT-2020.TECH PERF REQ] - Minimum requirements related to technical performance for IMT-2020 radio interface(s). [Online]. Available: https://www.itu.int/md/R15-SG05-C-0040/en. Accessed on: Feb. 23, 2017.

[4] D. Choudhury, "5G wireless and millimetre wave technology evolution: An overview," in Proc. IEEE MTT-S Int. Microw. Symp. Dig., May 2015, pp. 1–4.

[5] L. Wei, R. Q. Hu, Y. Qian, and G. Wu, "Key elements to enable millimetre wave communications for 5G wireless systems," Wireless Commun., vol. 21, no. 6, pp. 136–143, Dec. 2014.

[6] A. Swindlehurst, E. Ayanoglu, P. Heydari, and F. Capolino, "Millimetre-wave massive MIMO: The next wireless revolution?" IEEE Commun. Mag., vol. 52, no. 9, pp. 56–62, Sep. 2014.

[7] T. S. Rappaport, F. Gutierrez, E. Ben-Dor, J. N. Murdock, Y. Qiao, and J. I. Tamir, "Broadband millimetre-wave propagation measurements and models using adaptive-beam antennas for outdoor urban cellular communications," IEEE Trans. Antennas Propag., vol. 61, no. 4, pp. 1850–1859, Apr. 2013.

[8] J.-S. Rieh, D. Yoon, and J. Yun, "An overview of solid-state electronic sources and detectors for Terahertz imaging," in Proc. 12th IEEE Int. Conf. Solid-State Integr. Circuit Technol., Oct. 2014, pp. 1–4.

[9] J. A. Nanzer, P. T. Callahan, M. L. Dennis, and T. R. Clark Jr., "Photonic signal generation for millimetre-wave communications," Johns Hopkins APL Tech. Dig., vol. 30, no. 4, pp. 299–308, Jan. 2012.

[10] T. Nagatsuma and K. Kato, "Photonically-assisted 300-GHz wireless link for real-time 100-Gbit/s transmission," in Proc. IEEE MTT-S Int. Microw. Symp., Jun. 2014, pp. 1–4.

[11] A. Stohr, "Photonic millimetre-wave generation and its applications in high data rate wireless access," in Proc. IEEE Top. Meeting Microw. Photon., Dec. 2010, pp. 7–10.

[12] T. Nagatsuma, "Photonic generation of millimetre waves and its applications," in Proc. Opt. Fiber Commun. Conf., 2012, Paper OM2B.7.

[13] Z. Jia, J. Yu, G. Ellinas, and G.-K. Chang, "Key enabling technologies for optical–wireless networks: Optical millimetre-wave generation, wavelength reuse, and architecture," J. Lightw. Technol., vol. 25, no. 11, pp. 3452–3471, Dec. 2007.

[14] H. Ito, T. Furuta, S. Kodama, and T. Ishibashi, "InP/InGaAs uni-travelling-carrier photodiode with 310 GHz bandwidth," *Electron. Lett.*, vol. 36, no. 21, pp. 1809–1810, Oct. 2000.

[15] T. Nagatsuma *et al.*, "Terahertz wireless communications based on photonics technologies," *Opt. Express*, vol. 21, no. 20, pp. 23736–23747, 2013.

[16] H.-W. Hubers, "Terahertz heterodyne receivers," *IEEE J. Sel. Top. Quantum Electron.*, vol. 14, no. 2, pp. 378–391, Apr. 2008.

[17] C. C. Renaud, M. J. Fice, L. Ponnampalam, M. Natrella, C. Graham, and A. J. Seeds, "Uni-travelling carrier photodetectors as THz detectors and emitters," *Proc. SPIE*, vol. 9370, Aug. 2015.

[18] H. Ito, S. Kodama, Y. Muramoto, T. Furuta, T. Nagatsuma, and T. Ishibashi, "High-speed and high-output InP-InGaAs unitraveling-carrier photodiodes," *IEEE J. Sel. Top. Quantum Electron.*, vol. 10, no. 4, pp. 709–727, Oct. 2004.

[19] N. Guo, "60-GHz millimetre-wave radio: Principle technology and new results," *EURASIP J. Wireless Commun. Netw.*, vol. 2007, no. 1, Jan. 2007, Art. no. 068253.

[20] Z. Pi and F. Khan, "An introduction to millimetre-wave mobile broadband systems," *IEEE Commun. Mag.*, vol. 49, no. 6, pp. 101–107, Jun. 2011.

[21] A. W. Mohammad *et al.*, "1 Gbaud QPSK wireless receiver using an opto-electronic mixer," in *Proc. IEEE Top. Meeting Microw. Photon.*, Oct. 2017, pp. 1–3.

[22] F. van Dijk *et al.*, "Integrated InP heterodyne millimetre wave transmitter," *IEEE Photon. Technol. Lett.*, vol. 26, no. 10, pp. 965–968, Mar. 2014.

[23] M. Natrella, E. Rouvalis, C.-P. Liu, H. Liu, C. C. Renaud, and A. J. Seeds, "InGaAsP-based uni-travelling carrier photodiode structure grown by solid source molecular beam epitaxy," *Opt. Express*, vol. 20, no. 17, pp. 19279–19288, 2012.

[24] E. Rouvalis, M. J. Fice, C. C. Renaud, and A. J. Seeds, "Optoelectronic detection of millimetre-wave signals with travelling-wave uni-travelling carrier photodiodes," *Opt. Express*, vol. 19, no. 3, pp. 2079–2084, 2011.

[25] R. Sobot, "Electrical noise: solutions," in *Wireless Communication Electronics by Example*. Berlin, Germany: Springer, 2014, ch. 15, p. 135.

[26] H. Shams, M. J. Fice, K. Balakier, C. C. Renaud, F. van Dijk, and A. J. Seeds, "Photonic generation for multichannel THz wireless communication," *Opt. Express*, vol. 22, no. 19, pp. 23465–23472, 2014.

[27] H. Friis, "Noise figures of radio receivers," *Proc. IRE*, vol. 32, no. 7, pp. 419–422, 1944.

Chin-Pang Liu (M'10) received the B.Eng. (Hons.) and Ph.D. degrees in electronic and electrical engineering from University College London, London, U.K., in 1994 and 2000, respectively. His Ph.D. thesis was concerned with optoelectronic mixing using heterojunction bipolar transistors.

He is currently a Senior Lecturer with University College London. His research interests include photonic devices, wireless and optical communications, and photonic sampling.

Chris Graham received the B.Eng. degree from the University of Essex, Colchester, U.K, and the Ph.D. degree, in 2011, with research in ultrafast photonic switches for sampling applications. In 2006, he joined the Ultrafast Photonics Group, Department of Electronic and Electrical Engineering, University College London. Has was a Research Associate with the Photonics Group for the last seven years working in the fields of uni-traveling photodiode design fabrication and evaluation, photonic integrated circuit packaging, and ultrafast photoconductors. His is the author or coauthor of more than 20 publications in peer-reviewed journals and international conferences, and he holds one patent.

Michele Natrella received the five-year Laurea degree in electronic engineering from Politecnico di Bari, Bari, Italy, in 2006, and the Ph.D. degree in photonics in 2015. He spent a year in the industry as a Design Engineer within the electronic security systems sector. He was then a Research Engineer with the Applied Research Organisation CETMA, Brindisi, Italy. Here, he spent three years conducting research on wireless communications, laser range finders, and software development. He moved to academia in October 2010, when he joined the Ultrafast Photonics Group, University College London, London, U.K., as a Marie Curie Researcher, to work on the development of photonic terahertz emitters and receivers. His research in academia has led to 21 publications in peer-reviewed journals and international conferences.

Ahmad Wasfi Mohammad received a five-year degree in electrical engineering (telecom and computer) from Birzeit University, Palestine, in 2012, and the Erasmus Mundus Scholarship for Master's degree in photonic networks engineering (MAPNET), during which he studied at Aston University, Birmingham, U.K., Scuola Superiore Sant'Anna, Pisa, Italy, and the Technical University of Berlin, Berlin, Germany. Since 2016, he has been working toward the Ph.D. degree at University College London, London, U.K. For one year, he was with the Consolidated Contractors Company, as an Electrical Engineer. In 2016, he was with the Ultrafast Photonics Group, University College London, as a Marie-Curie Early Stage Researcher within the European Project FiWiN5G. His current research focuses on photonic integrated circuits for millimeter wave transmitters and receivers.

Alwyn J. Seeds (F'97) received the B.Sc., Ph.D., and D.Sc. degrees from the University of London, London, U.K. After working as a Staff Member with Lincoln Laboratory, Massachusetts Institute of Technology, he moved to London, where he is currently the Head of the Photonics Group, University College London. He is the author or coauthor of more than 400 papers. He co-founded Zinwave, a manufacturer of wireless over fiber systems, now a unit of McWane Inc. He is a Fellow of the Royal Academy of Engineering (U.K.). His IEEE roles have included Chair of the Lightwave Technical Committee, MTT-S, and Vice-President for Technical Affairs, Photonics Society.

Haymen Shams (S'09–M'12) received the M.Sc. degree from the Electronic and Electrical Department, Alexandria University, Alexandria, Egypt, in 2006, and the Ph.D. degree in electrical and electronic engineering from Dublin City University, Dublin, Ireland, in 2011. His Ph.D. dissertation addressed the optical technologies for generation and distribution of millimeter waves and ultrawideband RF signals in radio over fiber systems. After the Ph.D. degree, he was a Postdoctoral Researcher with the Photonics Group, Tyndall National Institute, University College Cork, for two years. He is currently a Senior Research Associate with the Photonic Group, Department of Electrical and Electronic Engineering, University College London, London, U.K. He is the author or coauthor of more than 60 peer-reviewed journals and conference papers. His research interests include RF-over-fiber for wireless communication including ultrawideband and millimeter wave signals, digital coherent receivers, digital signal processing, optical coherent THz, and spectroscopy.

Cyril C. Renaud (M'08–SM'12) received the Engineering degree from the Ecole Superieure d'Optique, Orsay, France, and the Diplome d'Etudes Approfondies in optics and photonics from the University Paris XI, Orsay, France, in 1996, and the Ph.D. degree in 2001. For one year, he was a Project Engineer with Sfim-ODS, working on the development of microchips lasers and portable range finders. He then joined the Optoelectronics Research Centre, University of Southampton, Southampton, U.K., in 1998, to work on diode pumped high-power ytterbium-doped fiber-lasers, with particular interest on Q-switched system and 980-nm generation. He is currently a Reader in photonics at the University College London (UCL), London, U.K., and the UCL Site Director for the UCL/Cambridge Doctoral Training Centre in Integrated Photonic and Electronic Systems. His is the author or coauthor of more than 140 peer-reviewed journals and international conferences, and he holds three patents.